Contents lists available at UGC-CARE

International Journal of Pharmaceutical Sciences and Drug Research

[ISSN: 0975-248X; CODEN (USA): IJPSPP]

journal home page : http://ijpsdronline.com/index.php/journal

Research Article

Green Synthesis of Zinc Oxide Nanoparticles using *Peristrophe bicalyculata* (Retz.) Nees Leaf Extract: Characterization and Antibacterial Activity

Jigisha Darji[1*], Kaushik Patel[1], Kaushik Jodhani[2]

[1]*Department of Botany, Smt. S. M. Panchal Science College, Talod, Sabarkantha, Gujarat, India.*
[2]*Department of Botany, BRD School of Biosciences, Vadtal Road, Vallabh Vidyanagar, Anand, Gujarat, India.*

ARTICLE INFO

Article history:
Received: 04 May, 2025
Revised: 24 June, 2025
Accepted: 30 June, 2025
Published: 30 July, 2025

Keywords:
Biosynthesis, Peristrophe bicalyculata, ZNO nanoparticles, Antibacterial activity

DOI:
10.25004/IJPSDR.2025.170406

ABSTRACT

Nanotechnology has developed as a key part of investigation in modern-day material science in recent decades. Biosynthesized nanoparticles garnered substantial significance due to their accelerated synthesis, economic viability and environmentally benign characteristics. The current study uses Peristrophe bicalyculata (Retz.) Nees leaf extract to produce ZNO NPs in an ecologically safe manner. These nanoparticles were created using zinc acetate dihydrate, utilizing the extract of leaves as a biological reductant. Created nanoparticles were evaluated using UV-Visible (UV-VIS) spectroscopy. Characteristics of produced nanoparticles and their constituent elements were analysed through XRD (X-ray diffraction). The ZNO NPs exhibited crystalline morphology. According to SEM imaging, the ZNO NPs appeared to possess a non-uniform spheroid morphology. The functional groups involved in capping, along with reduction processes, were identified using Fourier transform infrared (FTIR) spectroscopy. Efficacy of ZNO-NPs may be associated with their size and shape as observed through scanning electron microscope (SEM) as well as transmission electron microscope (TEM). Our investigation assessed the efficiency of ZNO-NPs as potent bactericidal agents against Escherichia coli, Staphylococcus aureus, Salmonella typhi, Bacillus subtilis, Bacillus megaterium, Bacillus albus and Streptococcus pneumoniae. This study demonstrates that zinc oxide nanoparticles synthesized via a green approach possess intrinsic antibacterial efficacy, supporting their potential application in the development of antimicrobial therapeutics. Additional studies are essential to explore the mechanistic pathways and determine the cytotoxicity of zinc oxide nanoparticles.

INTRODUCTION

Nanotechnology is a rapidly evolving field focused on creating new materials at the nanoscale level. This field involves the synthesis, characterization and manipulation of matter at a size of 1 to 100 nm.[1] High surface-to-volume proportion is a special characteristic of NPs that makes them especially intriguing. This characteristic makes nanoparticles more sensitive as compared with bulk substances since atoms in the center are often less active as compared with atoms on the surface.[2] Research has indicated that a nanoparticle's surface-to-volume ratio increases with declining size, leading to increased antimicrobial potency.[3] Biological, physical, along chemical approaches can be utilized to fabricate nanoparticles.[4] Despite their effectiveness, these Approaches are resource-intensive, time-intensive and environmentally hazardous because they employ hazardous chemicals as reductants and stabilizing agents during the nanoparticle formation process, which has a number of negative consequences on the surroundings and living things.[5-7] Compared to conventional chemical or physical processes, green chemistry approaches for producing nanoparticles from plant extracts are more financially sustainable and environmentally benign

***Corresponding Author:** Mrs. Jigisha Darji
Address: Department of Botany, Smt. S. M. Panchal Science college, Talod-383215, Sabarkantha, Gujarat, India.
Email ✉: rathodjigisha096@gmail.com
Tel.: +91-9265249408

Relevant conflicts of interest/financial disclosures: The authors declare that the research was conducted in the absence of any commercial or financial relationships that could be construed as a potential conflict of interest.

because they are carried out at room temperature and physiological pH.[8] Various biological sources, including yeast, bacteria, actinobacteria, algae and plants, are utilized for NP synthesis. Among these sources, plants are regarded as the most suitable candidates for the synthesis of metal nanoparticles.[9] The phytochemicals, especially secondary metabolites such as alkaloids, tannins, terpenoids, and flavonoids of the plant extract, can function as reductants, facilitating the conversion of metal salts into nanoscale metallic particles.[10,11] This method also contributes to extending the life span of nanoparticles.[12]

The utilization of metallic/metal oxide nanoscale particles, including silver, aluminum oxide, iron oxide and zinc oxide, is steadily increasing over time.[13] Researchers are particularly interested in zinc oxide nanoparticles amongst various metal oxide NPs due to their many uses in solar cells, electronics, communications, sensors, photocatalytic degradation, cosmetics, ecosystem preservation and biological and medical fields. These applications are made possible by their advantageous properties, which include minimal cell damage, biological safety and economic efficiency.[14-17] Furthermore, there are numerous biological uses for zinc oxide nanoparticles, such as biosensing, bio-labelling, gene and medication delivery, cancer therapy advancements, the agricultural sector, and nanomedicines.[18-20] Furthermore, the USFDA has acknowledged ZNO as a highly stable material.[21] Zinc oxide exhibits an energy band gap of 3.3 eV and generates OH ions at elevated concentrations than many other nanoparticles upon reaction, contributing to its bioactivity.[22] Factors including particle diameter, concentration, morphological characteristics, as well as specific surface area, substantially impact the antimicrobial effectiveness of zinc oxide NPs. Research has indicated that antimicrobial activity increases as particle size decreases from bulk zinc oxide to smaller zinc oxide particles. High concentration of H_2O_2 produced on the surface of ZNO NPs is the main cause of their antibacterial potency.[23] ZNO NPs kill bacteria by binding to their cell surfaces and interfering with membrane permeability. Once they get into the cell, they trigger oxidative stress, which stops the cell proliferation thus eventually kill them.[24]

Peristrophe bicalyculata, belonging to the genus *Peristrophe* in the family Acanthaceae, is an erect shrub with a slender, branched stem, growing to a height of 30 to 70 cm.[25] This erect shrub originates from tropical regions of Africa, extending to Nigeria as well as Niger from Mauritania, and is also found in parts of Asia, including India, Burma and Thailand. It is usually denoted to as the "Goddess of mercy".[26] In traditional medicine, it is used as an antivenom, applied for the treatment of skeletal fractures, ligament injuries, fever, cold, respiratory irritation, bronchial asthma, cardiovascular diseases and for treating various skin problems, as well as eye and ear infections.[27-29] The plant's leaves are applied for pain relief, fever suppression, inflammation reduction, cancer prevention, fertility-promoting and preventing diarrhea.[30] The herb also exhibits antibacterial properties (tuberculostatic).[31] The investigation was designed to synthesize zinc oxide nanoparticles employing *P. bicalyculata* (Retz.) Nees leaf extract characterizes the fabricated nanoparticles and evaluates antimicrobial efficacy targeting some gram-negative, in addition to gram-positive pathogenic microbes affecting humans. Synthesized zinc oxide NPs were investigated through UV-visible spectroscopy (UV-vis), Fourier transform infrared (FTIR), transmission electron microscopy (TEM), X-ray diffraction (XRD), and scanning electron microscopy (SEM).

Materials And Methods

Peristrosphe bicalyculata (Retz.) Nees (Acanthaceae) was collected from Sankleshwari hill, Banaskantha. HiMedia Laboratories Pvt. Ltd. (Mumbai) supplied the sodium hydroxide, zinc acetate dihydrate, and other chemicals. Bacterial strains were purchased from IMTECH, Chandigarh, India.

Plant Extract Preparation

The leaves were properly cleaned multiple times using distilled H_2O to eliminate dust as well as debris. Leaves were permitted to dry for 15 to 20 days at ambient temperature in the shade. Dried leaves were then crushed to yield coarse powder. About 5 g of powder was weighed, then boiled using 50 mL of double-distilled H_2O for 15 minutes. Once cooled, this aqueous extract was subjected to filtration using filter paper (Whatman #1). This extract was preserved at 4°C for later examination. For future use, the dried powder was kept at ambient temperature in a hermetically sealed container.

Biogenic Synthesis of ZNO NPs

15ml of extract of the plant was heated for 10 min at 50°C and 50 mL of 50 mM zinc acetate dihydrate solution was gradually added drop by drop with constant stirring. The mixture was held at a stable pH 9. The mixture was reduced completely by heating it to 95°C for 30 minutes. A cream-colored, yellow precipitate of zinc hydroxide was generated from the reaction solution. After centrifuging the precipitates for 20 minutes at 4°C at 13,000 rpm, it was twice cleaned with sterile de-ionized water. Using a hot air oven, the zinc oxide nanoparticle powder was dried for 24 hours at 70°C.

Evaluation of zinc oxide nanoparticles

A Shimadzu UV-1800 UV-vis spectrophotometer (Shimadzu Corporation, Japan) was utilized to record UV-VIS light spectra of ZNO NPs at diverse wavelengths between 300 and 700 nm.

FTIR was performed on dried ZNO NP powder with the help of Nicolet 6700 Fourier Transform Infrared

Spectrophotometer (Thermo Fisher Scientific) in the 4000 to 400 cm^{-1} range.

XRD of ZNO nanoparticles was performed with the help of an X-ray diffractometer (model D8 Advance, Bruker, Germany), in the 2θ range from 20 to 80°.

FESEM combined with X-ray spectroscopy (EDAX) was utilized to observe the surface features of produced ZNO NPs utilizing a Nova Nano FEG-SEM 450 (FEI Ltd, Netherlands). HRTEM was utilized to examine morphological characteristics and size dispersion of ZNO NPs using a Talos F200i S/TEM (HRTEM-200KV) (Thermo Fisher Scientific).

Antimicrobial Assay

Antibacterial potential of produced ZNO NPs was assessed with the help of agar well diffusion approach, with minor modifications.[32] The test microorganisms were *Escherichia coli*, *Staphylococcus aureus*, *Salmonella typhi*, *Bacillus subtilis*, *Acinetobacter baumannii* and *Streptococcus pneumoniae*. With a sterilized glass spreader, 100 µL aliquots of bacterial suspension at a concentration of 106 CFU per mL were evenly distributed on nutrient agar plates. Each plate had three wells 3 mm in radius, formed with a sterile cork borer. Aliquots of 100 µL of multiple concentrations (1, 3, 5, 10, 20 and 30 mg permL) of ZNO NPs solutions were poured into corresponding wells. The positive control was ciprofloxacin (5 mg/mL), while the negative control was sterile distilled water. Also, aqueous plant extract was poured to compare the antibacterial activity. To make sure the samples were homogeneously dispersed throughout the nutrient agar, plates were incubated for 24 hours at 37°C after being refrigerated for 30 minutes. Measurements and records were made of the radius of the bacterial growth inhibition zone. Three separate runs of the experiment were made.

Results And Discussion

Structural Analysis

Biofabricated ZNO NPs were investigated through XRD analysis in the 2θ range of 20 to 80°. The XRD spectrum of green synthesized ZNO NPs is displayed in Fig. 1. Lattice planes (202), (004), (201), (112), (200), (103), (110), (102), (101), (002), and (100) were represented by diffraction peaks that were found at 2θ values of 76.94°, 72.52°, 69.07°, 67.94°, 66.38°, 62.85°, 56.59°, 47.52°, 36.25°, 34.40°, and 31.75° sequentially. According to the Joint Committee on Powder Diffraction Standards (JCPDS file: 36-1451), this peak displays the wurtzite hexagonal structure of ZNO and verifies the presence of ZNO Nps.[33] Narrow and sharp XRD peaks validated the great crystallinity of the produced zinc oxide NPs.[34] Demissie *et al*., achieved similar results by synthesizing ZNO NPs utilizing leaf extract from *Lippia adoensis*.[35] They observed diffraction peaks at 69.96°, 67.97°, 66.41°, 62.86°, 56.59°, 47.54°, 36.24°, 34.42°, and 31.76°, which correspond to (201), (112), (200), (103), (110), (102), (101), (002), and (100). The computed size and lattice strain values for ZNO NPs are accessible in Table 1. Dimensions of nanoparticles were determined by applying Debye-Scherrer's equation, which is expressed as

$$D = \frac{0.94\lambda}{\beta cos\theta}$$

Where β is for full width at half maximum (FWHM), θ stands for Bragg's angle, λ for X-ray wavelength, and D for crystalline size. The intense plane of (101) showed that ZNO NPs produced showed 41.13 nm average crystalline size.

Optical Characterization

UV – visible absorption

To authenticate the generation of the ZNO NPs, UV-vis spectroscopy was conducted within the 300 to 700 nm spectral range. An absorbance peak was noticed at 375 nm in the UV-vis spectral analysis of produced ZNO NPs (Fig. 2). The Detected peak value falls within the 360 to 380 nm range, which is indicative of zinc oxide nanoparticle absorption. Rahaiee *et al*. reported a similar outcome, with a significant peak discovered at 370 nm.[36] An absorption peak of 375 nm was found as per an investigation led by Mahalaxmi *et al*., of the formation of ZNO NPs mediated by *Sesbania grandiflora*.[37] Using the following formula, the ZNO energy gap at the highest absorption peak was determined to be 3.3 eV.[38]

$$Eg = \frac{hv}{\lambda} = \frac{1239.83}{\lambda}$$

Here λ denotes the wavelength of maximum absorption; E_g stands for the bulk band in eV; v is the speed of light; h denotes Planck's constant.

Fourier transform infrared spectroscopy (FTIR)

FTIR investigation offers molecular evidence on the chemicals as well as biomolecules in plant extract, which are involved in the manufacturing of NPs by identifying the functional groups on their surface. In this investigation, an FTIR investigation was conducted between 4000 to 400 cm^{-1}. Fig. 3 displays infrared absorption spectra of ZNO NPs made from the extract of leaves of *P. bicalyculata*. O-H stretching vibration of alcohols involved in hydrogen bonding and the isolated hydroxyl stretch characteristic of the phenol group are characterised by absorption at 3552 cm^{-1}. IR signal at 3479 cm^{-1} shows the medium-intensity N-H bond stretch associated with a primary amine and the hydroxyl group vibration characteristic of alcohols. The vibrational stretching of the hydroxyl group in alcohols accounts for the absorption peak at 3414 cm^{-1}. Peak at 3233

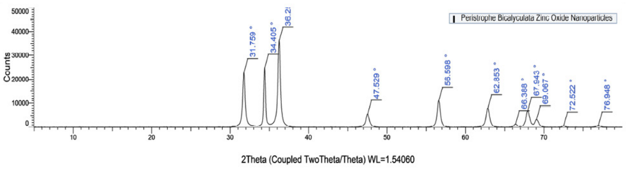

Fig. 1: XRD spectra of *Peristrophe bicalyculata* leaf-extract mediated zinc oxide nanoparticles

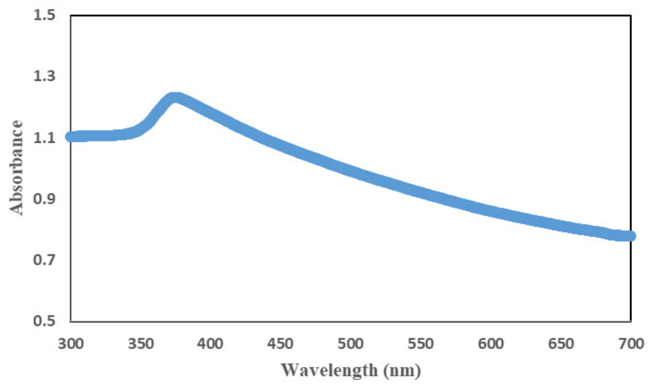

Fig. 2: UV-vis spectral analysis of zinc oxide nanoparticles

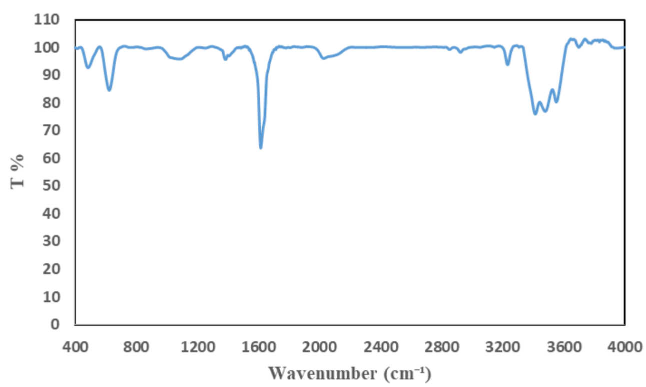

Fig. 3: FTIR spectra of zinc oxide nanoparticles derived from *P. bicalyculata* leaf extract

cm^{-1} results from alcoholic O-H stretch as well as carboxyl group vibrations. Absorption bands at 2925 as well as 2853 cm^{-1} relate to the hydroxyl stretching vibration of carboxyl acid along with alcohol, the stretching vibration of the amino group in amine salts and the C-H stretching of alkanes. The vibrational band that appeared at 2028 cm^{-1} is attributed to stretching vibrations of the N=C=S moiety in isothiocyanate and the C=C=N group in ketenimine. The 1616 cm^{-1} band is characteristic of the conjugated C=C bond stretch, cyclic alkenes, α, β-unsaturated ketones, along with N-H bending vibrations in amine groups. Medium 1385 cm^{-1} peak arises from C-H bending vibration of aldehyde and O-H bending vibrations of alcohol, as well as phenol. Absorbance at 1074 cm^{-1} specifies the vibrational stretch of the C-N linkage in amines. The resonance at 624 cm^{-1} is indicative of the vibrational mode of the C-Br bond in alkyl halides with medium intensity. The absorption band confirms the existence of ZNO at 484 cm^{-1}.[39] Absorption bands between 1066 to 1250 cm^{-1} correspond to C-N stretching of aliphatic amines, indicative of proteins/enzymes. As reported by Khan *et al*., the vibrational bands between 3300 to 2500 per cm are attributed to O-H stretching of carboxylic acid.[40]

Table 1: Crystalline size and lattice strain of ZNO nanoparticles determined by X-ray diffraction (XRD) analysis

2θ (°)	*Crystalline size (nm)*	*Lattice strain*
31.75	48.34 (100)	0.0050
34.40	59.43 (002)	0.0035
36.25	41.13 (101)	0.0045
47.52	25.91 (102)	0.0043
56.59	24.75 (110)	0.0032
62.85	21.23 (103)	0.0031
66.38	20.25 (200)	0.0029
67.94	19.46 (112)	0.0029
69.06	18.58 (201)	0.0030
72.52	25.28 (004)	0.0020
76.94	17.31 (202)	0.0027

Microscopic Analysis

Scanning electron microscopy with energy dispersive X-ray (EDX)

The size, shape and surface area of produced ZNO NPs were investigated through SEM-EDX characterization. The produced ZNO NPs have an asymmetrical spherical structure, exhibiting similarity to that described by Alamdari *et al*., as illustrated in the SEM micrograph of Fig. 4a.[41] The image displays clustered zinc oxide nanoparticles as well as an unevenly formed microstructure that resembles a flower. The enhanced surface area and persistent intermolecular interactions of biomediated nanoparticles contribute to their propensity for agglomeration.[42] EDX examination of the produced nanoparticles demonstrates that oxygen and zinc are present as their constituent elements. For the ZNO nanoparticles produced by *P. bicalyculata*, the elemental analysis reveals 78.25% zinc and 21.75% oxygen components (Fig. 4b).

Transmission electron microscopy

Fig. 5 illustrates the spherical and flower-shaped structure of ZNO NPs as seen in acquired TEM micrographs. The average size of ZNO nanoparticles was found to be around 30 nm, which is similar to the value described by Dhandapani *et al*. [43]. Additionally, the TEM scans showed that the nanoparticles were clumped together. Surrounding the ZNO NPs, there are biomolecules in the plant extract that may be responsible for this aggregation.

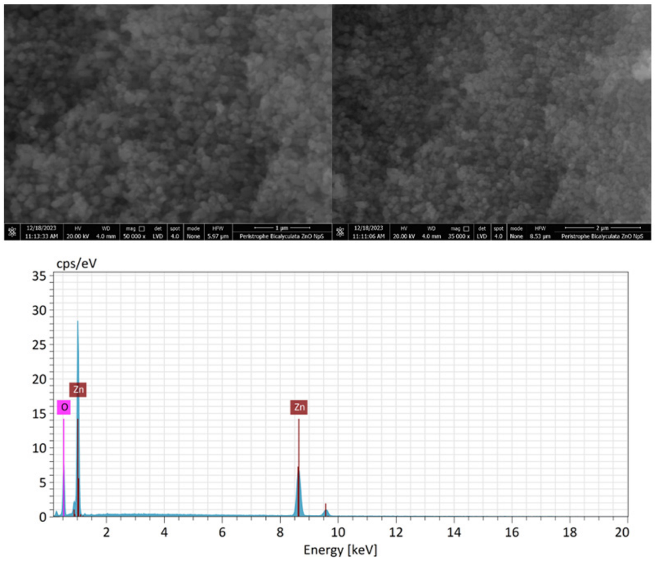

Fig. 4: (a) SEM micrograph of *P. bicalyculata* leaf extract-derived zinc oxide nanoparticles (b) EDX spectral data for *P. bicalyculata* leaf extract-derived zinc oxide nanoparticles

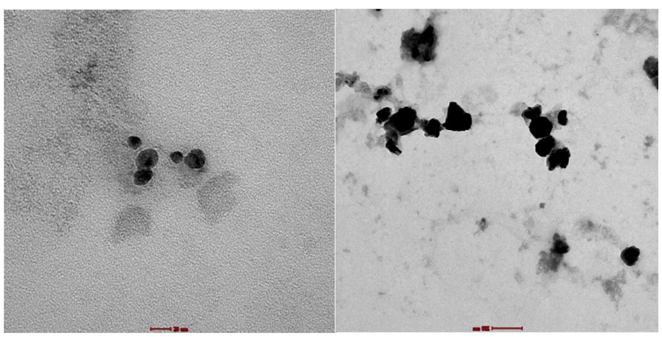

Fig. 5: Transmission electron microscopy (TEM) image of synthesized zinc oxide nanoparticles

Assessment of the Bacterial inhibition capability of biosynthesized zinc oxide nanoparticles

The agar well diffusion assay was utilized to inspect the bactericidal efficacy of the produced zinc oxide nanoparticles targeting six pathogenic microorganisms. A range of nanoparticle concentrations (1, 3, 5, 10, 20 and 30 mg per mL) was poised and used. Antibacterial potency was measured targeting three gram-positive bacteria (*B. subtilis*, *S. aureus*, *S. pneumoniae*) and three gram-negative bacteria (*S. typhi*, *E. coli*, *A. baumannii*). Ciprofloxacin served as the standard reference for each bacterial strain. The antimicrobial properties of the formulated nanoparticles, which inhibit bacterial growth, are observed as a distinct inhibition zone, as represented in Fig. 6. Table 2 presents the inhibition outcomes of zinc oxide nanoparticles. With two exceptions, all bacterial strains were vulnerable to the action of the produced ZNO NPs. Zones of inhibition for *S. aureus* at 3, 5 and 30 mg per mL concentration were 10.33 ± 0.57, 11.66 ± 0.57 and 10.33 ± 0.57, respectively. The zones of inhibition for *B. subtilis* at 1, 3, 5, 10, 20 and 30 mg per mL concentration were 13.66 ± 0.57, 11 ± 1, 14.33 ± 1.15, 26.66 ± 0.57, 26.66 ± 0.57 and 29.66 ± 0.57, respectively. The value zone of inhibition for *A. baumannii* at 10, 20 and 30 mg per mL concentration was 10.33 ± 0.57. The value of zone of inhibition for *S. pneumoniae* at 3, 5 and 20 mg per mL concentration was 10.33 ± 0.57, 10.33 ± 0.57 and 10.66 ± 0.57, respectively. *B. subtilis* had a significant zone of inhibition (mean value) of 29.66 ± 0.57 mm, indicating greater susceptibility. In comparison to *B. subtilis*, *A. baumannii, S. aureus*, as well as *S. pneumoniae* demonstrated reduced susceptibility, with zones of inhibition of 11.66 ± 0.57, 10.33 ± 0.57, and 10.66 ± 0.57, respectively. *S. typhi* as well as *E. coli* did not show any susceptibility, with no zone of inhibition. The antibacterial performance of ZNO nanoparticles is well established in the literature. Farooq *et al*. assessed the antimicrobial potential of ZNO nanoparticles synthesized by *Calotropis gigantea* flower, stem and leaf extract targeting *B. subtilis, P. multocida, E. coli*, and *S. aureus*.[44] Zinc oxide NPs synthesized using *Crotalaria verrucosa* were shown by Sana *et al*. to be effective against diverse disease-causing bacterial strains, including *P. vulgaris*, *S. aureus*, *E. coli*, as well as *K. pneumoniae*, with the greatest cytotoxic effects occurring at higher nanoparticle concentrations.[45] El-Belely *et al*. synthesized ZNO nanoparticles and assessed their antimicrobial efficacy targeting *P. aeruginosa*, *E. coli, C. albicans*, *B. subtilis*, as well as *S. aureus*.[46]

Nanoparticles possess antibacterial properties primarily due to their tiny size, which leads to a significantly higher surface area relative to volume. This intensified surface area enhances their interaction with microbial structures, allowing them to exert antibacterial effects. The reactive oxygen species (ROS) formation induced by NPs also contributes to their antibacterial effectiveness by disrupting bacterial cellular proteins and deoxyribonucleic acid. Moreover, bacteria have not yet developed highly effective resistance mechanisms against nanoparticles, further supporting their antibacterial efficacy.[47] Production of several reactive species, including hydroxide ion (OH-), hydrogen peroxide (H2O2), and superoxide radical (O2-), is responsible for the harmful effects that arise from ROS creation. These reactive species are produced when nanoparticles interact with hydroxyl groups and absorbed water (H_2O), leading to the formation of hydroxide ions and protons, which subsequently generate O^{2-}. The reaction of O^{2-} with H^+ results in the formation of hydroperoxyl radical (HO_2), which subsequently combines with electrons and protons to generate H_2O_2. The final product, H_2O_2, penetrates the microbial envelope, where it binds to lipids, proteins and nucleic acids, ultimately causing cellular apoptosis.[48] Zinc oxide nanoparticles are drawn to the cytoplasmic membrane of bacteria, resulting in damage to the bacterial genome. This ultimately results in microbial cell death due to the rupture of surface of cell.[36] Distinct cell wall structures of gram-negative as well as gram-positive

Table 2: Mean value of inhibition zone (mm) synthesized by zinc oxide nanoparticles generated by *P. bicalyculata* leaf extract

S/N	*Organism*	*Mean width of Inhibition zone (mm)*						
		Concentration of ZNONPs						*Ciprofloxacin*
		1 mg ml^{-1}	*3 mg ml^{-1}*	*5 mg ml^{-1}*	*10 mg ml^{-1}*	*20 mg ml^{-1}*	*30 mg ml^{-1}*	*5 mg ml^{-1}*
1	*E. coli*	0	0	0	0	0	0	49.66 ± 0.57
2	*S. aureus*	0	10.33 ± 0.57	11.66 ± 0.57	0	0	10.33 ± 0.57	28.33 ± 0.57
3	*S. typhi*	0	0	0	0	0	0	39.33 ± 1.15
4	*B. subtilis*	13.66 ± 0.57	11 ± 1	14.33 ± 1.15	26.66 ± 0.57	26.66 ± 0.57	29.66 ± 0.57	39.66 ± 0.57
5	*A. baumannii*	0	0	0	10.33 ± 0.57	10.33 ± 0.57	10.33 ± 0.57	29.33 ± 0.57
6	*S. pneumoniae*	0	10.33 ± 0.57	10.33 ± 0.57	0	10.66 ± 0.57	0	27.33 ± 0.57

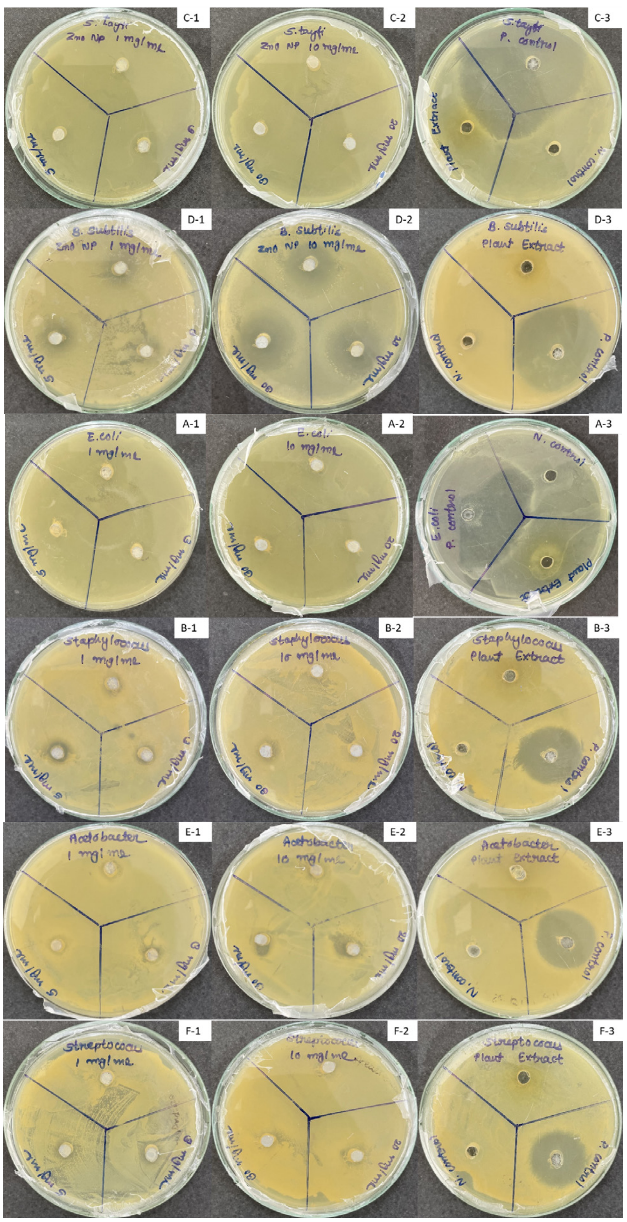

Fig. 6: Zone of inhibition of plant-mediated zinc oxide nanoparticles targeting (A) *E. coli* (B) *S. aureus* (C) *S. typhi* (D) *B. subtilis* (E) *A. baumannii* (F) *S. pneumoniae*

bacteria cause variations in the absorbability of reactive oxygen species (ROS).[49] In general, gram-negative species are less sensitive than gram-positive species owing to variations in their cell wall architecture. Gram-negative bacteria possess a thin (<10 nm) layer of peptidoglycan surrounded by an outer membrane that contains multiple pores. In contrast, gram-positive bacteria feature a dense (20–80 nm) peptidoglycan layer that serves as the cell exterior. Compared to gram-positive species, Gram-negative bacteria are less sensitive because they have an extra outer membrane.[50] The antibacterial efficiency improved as the particle diameter decreased from macro-scale ZNO to bio-fabricated white zinc oxide nanoparticles, indicating an opposite association amid antibacterial action as well as the size of the metallic oxides.[51] Another proposed mechanism highlights the relationship between the structural features of nanoparticles and their association with bacterial organisms. Smaller nanoparticles exhibit higher surface reactivity, allowing them to penetrate cells more easily and release Zn^{2+} ions. It is well known that Zn^{2+} released from ZNO nanoparticles interferes with bacterial physiological processes, active transport and catalytic efficiency, which in turn causes bacterial cell death.[39]

Conclusion

This study demonstrates that a sustainable and economical strategy is ideal for synthesizing spherical ZNO nanoparticles with strong antimicrobial properties using *P. bicalyculata* leaf extract. UV–vis analysis discovered a prominent absorption peak at 375 nm for synthesized NPs. Analysis of the ZNO nanoparticles was done with FTIR, XRD, SEM with EDAX, as well as TEM. The impact of multiple zinc oxide nanoparticle concentrations on infectious bacterial species was assessed. High concentration of zinc oxide nanoparticles (30 mg/ml) successfully inhibited the development of bacteria. A higher concentration resulted in a larger zone of inhibition, indicating an enhanced antibacterial effect. This study holds significant social significance as a consequence of the biocompatible and cost-effective nature of the material, making it appropriate for the environment and biomedical applications.

Acknowledgment

The BRD School of Biosciences, Vadtal Road, Vallabh Vidyanagar, is acknowledged by the authors for providing the resources and assistance required to accomplish this study.

References

1. Pillai AM, Sivasankarapillai VS, Rahdar A, Joseph J, Sadeghfar F, Rajesh K, Kyzas GZ. Green synthesis and characterization of zinc oxide nanoparticles with antibacterial and antifungal activity. Journal of Molecular Structure. 2020 Jul 5; 1211:128107. Available from: https://doi.org/10.1016/j.molstruc.2020.128107
2. Jayachandran A, Aswathy TR, Nair AS. Green synthesis and characterization of zinc oxide nanoparticles using *Cayratia pedata* leaf extract. Biochemistry and Biophysics Reports. 2021 Jul 1; 26:100995. Available from: https://doi.org/10.1016/j.bbrep.2021.100995
3. feanyichukwu UL, Fayemi OE, Ateba CN. Green synthesis of zinc oxide nanoparticles from pomegranate (*Punica granatum*) extracts and characterization of their antibacterial activity. Molecules. 2020 Oct 2; 25(19):4521. Available from: https://doi.org/10.3390/molecules25194521
4. Imade EE, Ajiboye TO, Fadiji AE, Onwudiwe DC, Babalola OO. Green synthesis of zinc oxide nanoparticles using plantain peel extracts and the evaluation of their antibacterial activity. Scientific African. 2022 Jul 1; 16:e01152. Available from: https://doi.org/10.1016/j.sciaf.2022.e01152
5. Vijayakumar S, Mahadevan S, Arulmozhi P, Sriram S, Praseetha PK. Green synthesis of zinc oxide nanoparticles using *Atalantia monophylla* leaf extracts: Characterization and antimicrobial analysis. Materials Science in Semiconductor Processing. 2018 Aug 1; 82:39-45. Available from: https://doi.org/10.1016/j.mssp.2018.03.017
6. Abdelbaky AS, Abd El-Mageed TA, Babalghith AO, Selim S, Mohamed AM. Green synthesis and characterization of ZNO nanoparticles using *Pelargonium odoratissimum* (L.) aqueous leaf extract and their antioxidant, antibacterial and anti-inflammatory activities. Antioxidants. 2022 Jul 26; 11(8):1444. Available from: https://doi.org/10.3390/antiox11081444
7. Singh AK, Pal P, Gupta V, Yadav TP, Gupta V, Singh SP. Green synthesis, characterization and antimicrobial activity of zinc oxide quantum dots using *Eclipta alba*. Materials Chemistry and Physics. 2018 Jan 1; 203:40-8. Available from: https://doi.org/10.1016/j.matchemphys.2017.09.049
8. Abomuti MA, Danish EY, Firoz A, Hasan N, Malik MA. Green synthesis of zinc oxide nanoparticles using *salvia officinalis* leaf extract and their photocatalytic and antifungal activities. Biology. 2021 Oct 21; 10(11):1075. Available from: https://doi.org/10.3390/biology10111075
9. Umamaheswari A, Prabu SL, John SA, Puratchikody A. Green synthesis of zinc oxide nanoparticles using leaf extracts of *Raphanus sativus* var. Longipinnatus and evaluation of their anticancer property in A549 cell lines. Biotechnology Reports. 2021 Mar 1; 29:e00595. Available from: https://doi.org/10.1016/j.btre.2021.e00595
10. Jayachandran A, Aswathy TR, Nair AS. Green synthesis and characterization of zinc oxide nanoparticles using *Cayratia pedata* leaf extract. Biochemistry and Biophysics Reports. 2021 Jul 1; 26:100995. Available from: https://doi.org/10.1016/j.bbrep.2021.100995
11. Ramesh P, Saravanan K, Manogar P, Johnson J, Vinoth E, Mayakannan M. Green synthesis and characterization of biocompatible zinc oxide nanoparticles and evaluation of its antibacterial potential. Sensing and Bio-Sensing Research. 2021 Feb 1; 31:100399. Available from: https://doi.org/10.1016/j.sbsr.2021.100399
12. Alyamani AA, Albukhaty S, Aloufi S, AlMalki FA, Al-Karagoly H, Sulaiman GM. Green fabrication of zinc oxide nanoparticles using phlomis leaf extract: characterization and in vitro evaluation of cytotoxicity and antibacterial properties. Molecules. 2021 Oct 11; 26(20):6140. Available from: https://doi.org/10.3390/molecules26206140
13. Gur T, Meydan I, Seckin H, Bekmezci M, Sen F. Green synthesis, characterization and bioactivity of biogenic zinc oxide nanoparticles. Environmental Research. 2022 Mar 1; 204:111897. Available from: https://doi.org/10.1016/j.envres.2021.111897
14. Suresh J, Pradheesh G, Alexramani V, Sundrarajan M, Hong SI. Green synthesis and characterization of zinc oxide nanoparticle using insulin plant (*Costus pictus* D. Don) and investigation of its antimicrobial as well as anticancer activities. Advances in Natural Sciences: Nanoscience and Nanotechnology. 2018 Feb 2; 9(1):015008. Available from: DOI: 10.1088/2043-6254/aaa6f1
15. Al-darwesh MY, Ibrahim SS, Mohammed MA. A review on plant extract mediated green synthesis of zinc oxide nanoparticles and their biomedical applications. Results in chemistry. 2024 Jan 1; 7:101368. Available from: https://doi.org/10.1016/j.rechem.2024.101368
16. Rad SS, Sani AM, Mohseni S. Biosynthesis, characterization and antimicrobial activities of zinc oxide nanoparticles from leaf extract of *Mentha pulegium* (L.). Microbial pathogenesis. 2019 Jun 1; 131:239-45. Available from: https://doi.org/10.1016/j.micpath.2019.04.022
17. Aldalbahi A, Alterary S, Ali Abdullrahman Almoghim R, Awad MA, Aldosari NS, Fahad Alghannam S, Nasser Alabdan A, Alharbi S, Ali Mohammed Alateeq B, Abdulrahman Al Mohsen A, Alkathiri MA. Greener synthesis of zinc oxide nanoparticles: Characterization and multifaceted applications. Molecules. 2020 Sep 14; 25(18):4198. Available from: https://doi.org/10.3390/molecules25184198
18. Chikkanna MM, Neelagund SE, Rajashekarappa KK. Green synthesis of zinc oxide nanoparticles (ZNO NPs) and their biological activity. SN Applied Sciences. 2019 Jan; 1(1):117. Available from: https://doi.org/10.1007/s42452-018-0095-7
19. Bandeira M, Giovanela M, Roesch-Ely M, Devine DM, da Silva Crespo J. Green synthesis of zinc oxide nanoparticles: A review of the synthesis methodology and mechanism of formation. Sustainable chemistry and pharmacy. 2020 Mar 1; 15:100223. Available from: https://doi.org/10.1016/j.scp.2020.100223
20. Ahmed T, Wu Z, Jiang H, Luo J, Noman M, Shahid M, Manzoor I, Allemailem KS, Alrumaihi F, Li B. Bioinspired green synthesis of zinc oxide nanoparticles from a native *Bacillus cereus* strain RNT6: characterization and antibacterial activity against rice panicle blight pathogens *Burkholderia glumae* and *B. gladioli*. Nanomaterials. 2021 Mar 30; 11(4):884. Available from: https://doi.org/10.3390/nano11040884
21. Vijayakumar S, Krishnakumar C, Arulmozhi P, Mahadevan S, Parameswari N. Biosynthesis, characterization and antimicrobial activities of zinc oxide nanoparticles from leaf extract of *Glycosmis pentaphylla* (Retz.) DC. Microbial pathogenesis. 2018 Mar 1; 116:44-8. Available from: https://doi.org/10.1016/j.micpath.2018.01.003
22. Chunchegowda UA, Shivaram AB, Mahadevamurthy M, Ramachndrappa LT, Lalitha SG, Krishnappa HK, Anandan S, Sudarshana BS, Chanappa EG, Ramachandrappa NS. Biosynthesis of Zinc oxide nanoparticles using leaf extract of *Passiflora subpeltata*: Characterization and antibacterial activity against Escherichia coli isolated from poultry faeces. Journal of Cluster Science. 2021 Nov; 32:1663-72. Available from: https://doi.org/10.1007/s10876-020-01926-0
23. Sohail MF, Rehman M, Hussain SZ, Huma ZE, Shahnaz G, Qureshi OS, Khalid Q, Mirza S, Hussain I, Webster TJ. Green synthesis of zinc oxide nanoparticles by Neem extract as multi-facet therapeutic agents. Journal of Drug Delivery Science and Technology. 2020 Oct 1; 59:101911. Available from:
24. Abdelmigid HM, Hussien NA, Alyamani AA, Morsi MM, AlSufyani

NM, Kadi HA. Green synthesis of zinc oxide nanoparticles using pomegranate fruit peel and solid coffee grounds vs. chemical method of synthesis, with their biocompatibility and antibacterial properties investigation. Molecules. 2022 Feb 12; 27(4):1236. Available from: https://doi.org/10.1016/j.jddst.2020.101911

25. Arya P, Mehta JP. Antioxidant potential of Himalayan medicinal plants *Angelica glauca*, *Alysicarpus vaginalis* and *Peristrophe bicalyculata*. Int J Curr Microbiol App Sci. 2017; 6(7):1892-901. Available from: http://dx.doi.org/10.20546/ijcmas.2017.603.226
26. Abdulazeez MA, Jasim HA, Bashir M, Ross K, Fatokun AA. *Peristrophe bicalyculata* (Retz) Nees contains principles that are cytotoxic to cancer cells and induce caspase-mediated, intrinsic apoptotic death through oxidative stress, mitochondrial depolarisation and DNA damage. Biomedicine & Pharmacotherapy. 2022 Mar 1; 147:112597. Available from: https://doi.org/10.1016/j.biopha.2021.112597
27. Iwara IA, Mboso EO, Eteng OE, Elot KN, Igile GO, Ebong PE. *Peristrophe bicalyculata* extract and quercetin ameliorate high fat diet-streptozotocin-induced type ii diabetes in Wistar rats. Pharmacological Research-Modern Chinese Medicine. 2022 Mar 1; 2:100060. Available from: https://doi.org/10.1016/j.prmcm.2022.100060
28. Kalam MA, Naved M. CHAKSINI (PERISTROPHE BICALYCULATA (RETZ) NEES. : A COMPREHENSIVE REVIEW ON A LESSER-KNOWN HERB OF UNANI MEDICINE. Indian Journal of Unani Medicine. 2022 Jan; 15(1):27-32. Available from: https://doi.org/10.53390/IJUM.2022.15105
29. Arya PR. Antioxidant, phytochemical and antibacterial action of Himalayan medicinal herbs *Peristrophe bicalyculata* leaves extract against respiratory tract pathogens. Int J Pharm Pharm Sci. 2018; 10:16-21. Available from: http://dx.doi.org/10.22159/ijpps.2018v10i3.23961
30. Janakiraman N, Johnson M, Sahaya SS. GC–MS analysis of bioactive constituents of *Peristrophe bicalyculata* (Retz.) Nees. (Acanthaceae). Asian Pacific Journal of Tropical Biomedicine. 2012 Jan 1; 2(1):S46-9. Available from: https://doi.org/10.1016/S2221-1691(12)60128-2
31. Sheneni VD, Onoja AO, Edegbo E, Momoh TB. In-vitro antioxidant activities of *ocimum gratissimum*, *vitex doniana*, *carica papaya* and *peristrophe bicalyculata* using DPPH free radical scavenging activity. J. Nutr Health Food Eng. 2018; 8(6):371-5. Available from: https://doi.org/10.15406/jnhfe.2018.08.00298
32. Abdallah Y, Liu M, Ogunyemi SO, Ahmed T, Fouad H, Abdelazez A, Yan C, Yang Y, Chen J, Li B. Bioinspired green synthesis of chitosan and zinc oxide nanoparticles with strong antibacterial activity against rice pathogen *Xanthomonas oryzae* pv. *oryzae*. Molecules. 2020 Oct 19; 25(20):4795. Available from: https://doi.org/10.3390/molecules25204795
33. Álvarez-Chimal R, García-Pérez VI, Álvarez-Pérez MA, Arenas-Alatorre JÁ. Green synthesis of ZNO nanoparticles using a *Dysphania ambrosioides* extract. Structural characterization and antibacterial properties. Materials Science and Engineering: C. 2021 Jan 1; 118:111540. Available from: https://doi.org/10.1016/j.msec.2020.111540
34. Yassin MT, Mostafa AA, Al-Askar AA, Al-Otibi FO. Facile green synthesis of zinc oxide nanoparticles with potential synergistic activity with common antifungal agents against multidrug-resistant candidal strains. Crystals. 2022 May 26; 12(6):774. Available from: https://doi.org/10.3390/cryst12060774
35. Demissie MG, Sabir FK, Edossa GD, Gonfa BA. Synthesis of zinc oxide nanoparticles using leaf extract of *lippia adoensis* (koseret) and evaluation of its antibacterial activity. Journal of Chemistry. 2020; 2020(1):7459042. Available from: https://doi.org/10.1155/2020/7459042
36. Rahaiee S, Ranjbar M, Azizi H, Govahi M, Zare M. Green synthesis, characterization, and biological activities of saffron leaf extract-mediated zinc oxide nanoparticles: a sustainable approach to reuse an agricultural waste. Applied Organometallic Chemistry. 2020 Aug; 34(8):e5705. Available from: https://doi.org/10.1002/aoc.5705
37. PP V. In vitro biocompatibility and antimicrobial activities of zinc oxide nanoparticles (ZNO NPs) prepared by chemical and green synthetic route - a comparative study. BioNanoScience. 2020 Mar; 10(1):112-21. Available from: https://doi.org/10.1007/s12668-019-00698-w
38. Dangana RS, George RC, Agboola FK. The biosynthesis of zinc oxide nanoparticles using aqueous leaf extracts of *Cnidoscolus aconitifolius* and their biological activities. Green Chemistry Letters and Reviews. 2023 Jan 2; 16(1):2169591. Available from: https://doi.org/10.1080/17518253.2023.2169591
39. Ashwini J, Aswathy TR, Rahul AB, Thara GM, Nair AS. Synthesis and characterization of zinc oxide nanoparticles using *Acacia caesia* bark extract and its photocatalytic and antimicrobial activities. Catalysts. 2021 Dec 10; 11(12):1507. Available from: https://doi.org/10.3390/catal11121507
40. Khan AK, Renouard S, Drouet S, Blondeau JP, Anjum I, Hano C, Abbasi BH, Anjum S. Effect of UV irradiation (A and C) on *Casuarina equisetifolia*-mediated biosynthesis and characterization of antimicrobial and anticancer activity of biocompatible zinc oxide nanoparticles. Pharmaceutics. 2021 Nov 22; 13(11):1977. Available from: https://doi.org/10.3390/pharmaceutics13111977
41. Alamdari S, Sasani Ghamsari M, Lee C, Han W, Park HH, Tafreshi MJ, Afarideh H, Ara MH. Preparation and characterization of zinc oxide nanoparticles using leaf extract of *Sambucus ebulus*. Applied Sciences. 2020 May 23; 10(10):3620. Available from: https://doi.org/10.3390/app10103620
42. Karam ST, Abdulrahman AF. Green synthesis and characterization of ZNO nanoparticles by using thyme plant leaf extract. In Photonics 2022 Aug 22 (Vol. 9, No. 8, p. 594). MDPI. Available from: https://doi.org/10.3390/photonics9080594
43. Dhandapani KV, Anbumani D, Gandhi AD, Annamalai P, Muthuvenkatachalam BS, Kavitha P, Ranganathan B. Green route for the synthesis of zinc oxide nanoparticles from *Melia azedarach* leaf extract and evaluation of their antioxidant and antibacterial activities. Biocatalysis and Agricultural Biotechnology. 2020 Mar 1; 24:101517. Available from: https://doi.org/10.1016/j.bcab.2020.101517
44. Farooq A, Khan UA, Ali H, Sathish M, Naqvi SA, Iqbal S, Ali H, Mubeen I, Amir MB, Mosa WF, Baazeem A. Green chemistry based synthesis of zinc oxide nanoparticles using plant derivatives of *Calotropis gigantea* (giant milkweed) and its biological applications against various bacterial and fungal pathogens. Microorganisms. 2022 Nov 4; 10(11):2195. Available from: https://doi.org/10.3390/microorganisms10112195
45. Sana SS, Kumbhakar DV, Pasha A, Pawar SC, Grace AN, Singh RP, Nguyen VH, Le QV, Peng W. *Crotalaria verrucosa* leaf extract mediated synthesis of zinc oxide nanoparticles: Assessment of antimicrobial and anticancer activity. Molecules. 2020 Oct 23; 25(21):4896. Available from: https://doi.org/10.3390/molecules25214896
46. El-Belely EF, Farag MM, Said HA, Amin AS, Azab E, Gobouri AA, Fouda A. Green synthesis of zinc oxide nanoparticles (ZNO-NPs) using *Arthrospira platensis* (Class: Cyanophyceae) and evaluation of their biomedical activities. Nanomaterials. 2021 Jan 4; 11(1):95. Available from: https://doi.org/10.3390/nano11010095
47. Álvarez-Chimal R, García-Pérez VI, Álvarez-Pérez MA, Tavera-Hernández R, Reyes-Carmona L, Martínez-Hernández M, Arenas-Alatorre JÁ. Influence of the particle size on the antibacterial activity of green synthesized zinc oxide nanoparticles using *Dysphania ambrosioides* extract, supported by molecular docking analysis. Arabian Journal of Chemistry. 2022 Jun 1; 15(6):103804. Available from: https://doi.org/10.1016/j.arabjc.2022.103804
48. Abdo AM, Fouda A, Eid AM, Fahmy NM, Elsayed AM, Khalil AM, Alzahrani OM, Ahmed AF, Soliman AM. Green synthesis of Zinc Oxide Nanoparticles (ZNO-NPs) by *Pseudomonas aeruginosa* and their activity against pathogenic microbes and common house mosquito, *Culex pipiens*. Materials. 2021 Nov 18; 14(22):6983. Available from: https://doi.org/10.3390/ma14226983
49. Al Sharie AH, El-Elimat T, Darweesh RS, Swedan S, Shubair Z, Al-Qiam R, Albarqi H. Green synthesis of zinc oxide nanoflowers using *Hypericum triquetrifolium* extract: characterization, antibacterial activity and cytotoxicity against lung cancer A549 cells. Applied

Organometallic Chemistry. 2020 Aug; 34(8):e5667. Available from: https://doi.org/10.1002/aoc.5667
50. Taşdemir A, Aydin R, Akkaya A, Akman N, Altınay Y, Çetin H, Şahin B, Uzun A, Ayyıldız E. A green approach for the preparation of nanostructured zinc oxide: characterization and promising antibacterial behaviour. Ceramics International. 2021 Jul 15; 47(14):19362-73. Available from: https://doi.org/10.1016/j.ceramint.2021.03.273
51. Jayappa MD, Ramaiah CK, Kumar MA, Suresh D, Prabhu A, Devasya RP, Sheikh S. Green synthesis of zinc oxide nanoparticles from the leaf, stem and in vitro grown callus of *Mussaenda frondosa* L.: characterization and their applications. Applied nanoscience. 2020 Aug; 10:3057-74. Available from: https://doi.org/10.1007/s13204-020-01382-2

HOW TO CITE THIS ARTICLE: Darji J, Patel K, Jodhani K. Green Synthesis of Zinc Oxide Nanoparticles using *Peristrophe bicalyculata* (Retz.) Nees Leaf Extract: Characterization and Antibacterial Activity. Int. J. Pharm. Sci. Drug Res. 2025;17(4):354-362. **DOI:** 10.25004/IJPSDR.2025.170406